

Application of a Micro Nozzle Array Fuel Injector to Cold-Start Experiments of a 4 Stroke-cycle Gasoline Engine

Mikiya ARAKI*, Tomio OBOKATA, Tsuneaki ISHIMA and Seiichi SHIGA

Department of Mechanical Engineering

Gunma University

Kiryu, Gunma 376-8515 Japan

Masahiko MASUBUCHI and Tomojiro SUGIMOTO

Power Train Development Division

Toyota Motor Corporation

Susono, Shizuoka 410-1193 Japan

Abstract

Micro nozzle array ultrasonic fuel injectors (MNA injectors) were applied to cold start experiments of a 4 stroke cycle gasoline engine. In the MNA injector, a numerous number (order of 10^5) of micro nozzles (order of 10^{-6} m) are mounted on a thin nickel film. Gasoline is periodically pushed out at an ultrasonic frequency (order of 10^5 Hz), and a fine and uniform-diameter spray can be obtained. Two kinds of MNA injectors were applied to cold start experiments, whose nozzle exit diameter $d = 4$ and $6\ \mu\text{m}$, respectively. A conventional port fuel injector (PFI injector) was also applied for comparison. The Sauter mean diameters (SMDs) of the sprays are $15\ \mu\text{m}$ (for MNA, $d = 4\ \mu\text{m}$), $23\ \mu\text{m}$ (for MNA, $d = 6\ \mu\text{m}$), and $59\ \mu\text{m}$ (for PFI), respectively. An air cooled, single cylinder, 4 stroke cycle, gasoline engine was used for cold start experiments. The test engine is cranked using a cell motor, and the first ignition cycles after fuel injection start and the cumulative fuel amount before the first ignition were investigated at a wide range of the air fuel ratio A/F . For the MNA injector ($d = 4\ \mu\text{m}$), the first ignition cycles became much earlier when compared with the PFI injector, and the cumulative fuel amount during cranking reduced by about 30 %. It is shown that, by use of the MNA injector, the unburned hydrocarbon emissions during cold starting could be reduced.

Introduction

Fuel atomization is one of the key technologies to improve the emission characteristics of automotive engines. Up to 90 % of the unburned hydrocarbon (UHC) emissions from modern 4-stroke cycle gasoline engines occur during cold starting [1-4]. It is necessary to reduce the UHC emissions during cold starting in order to improve the overall emission characteristics of these engines. In port fuel injected (PFI) gasoline engines, the fuel is injected into the intake manifold, and some amount of the fuel impinges onto walls due to the spray penetration. During cold starting, due to the low temperature of the intake manifold and intake valves, the injected fuel adheres to the walls as liquid films, and the film thickness increases during the first 6 cycles after cranking start [1], and only 40 to 50 % of the fuel is introduced to the cylinder [2]. After entered the cylinder, some portion of the fuel adheres to the in-cylinder walls. When cold starting, in-cylinder fuel films do not fully vaporize even in the combustion process, and cumulates through several cycles [3, 4].

Since the air fuel ratio of the in-cylinder mixture becomes leaner than the flammable limit, it is necessary to increase the fuel injection amount during cold starting. The 'excess fuel' cannot be burned in the cylinder, and emitted from the exhaust valves. The catalytic converters are not activated during the first few seconds, and the excess fuel is emitted as UHCs from the tail pipe of the automobile. In order to reduce the UHC emissions during cold starting, it is necessary not only to activate the catalytic converters early as possible but also to improve the evaporation characteristics of the fuel. Therefore, improvement in the atomization characteristics of the fuel injector is the key to solve this problem.

The authors have proposed a new concept of a PFI gasoline injector, which uses micro nozzles and an ultrasonic oscillator [5-8]. A numerous number (order of 10^5) of micro nozzles (order of 10^{-6} m) [9] are machined on a

*Corresponding author

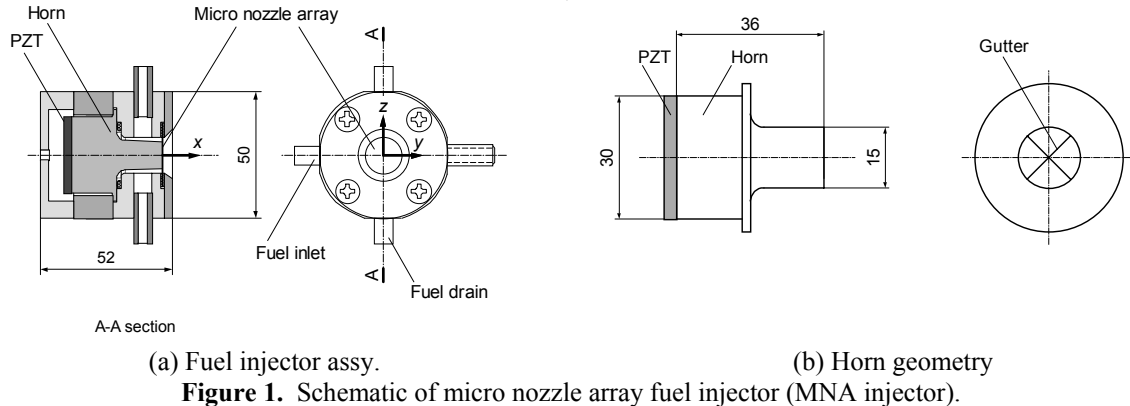


Figure 1. Schematic of micro nozzle array fuel injector (MNA injector).

thin nickel film. The fuel is periodically pushed out from the micro nozzles at an ultrasonic frequency (order of 10^5 Hz) using an ultrasonic oscillator [10]. Efficient atomization can be realized without high-pressure fuel pump and injectors. In previous studies [5-8], it is shown that fine uniform-diameter sprays can be obtained using the micro nozzle array (MNA injector).

In the present study, the MNA injectors [5-8] are applied to cold start experiments of a 4 stroke cycle gasoline engine. By use of two kinds of nozzle exit diameter d , two different fuel sprays whose Sauter mean diameter (SMD) is 15 and 23 μm are formed. Effect of spray diameter on the cold start characteristics of a 4 stroke cycle gasoline engine is investigated, experimentally. The test engine is cranked using a cell motor, and the first ignition cycles after fuel injection start and the cumulative fuel amount before the first ignition were investigated.

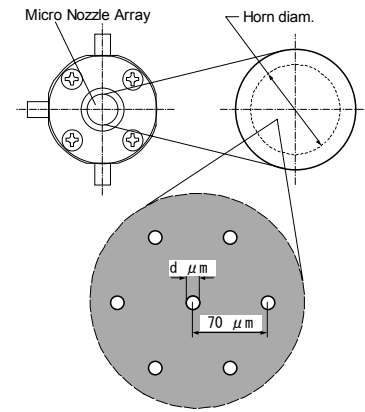


Figure 2. Schematic of micro nozzle array.

Experimental Setup and Procedure

Figure 1 shows a schematic of the MNA injector [5-8], which is consisted of a PZT (Lead zirconium titanate), a horn and the micro nozzle array. As the ultrasonic oscillator, a disk type PZT is used, whose diameter and thickness are 30 mm and 2.7 mm, respectively. High voltage is input to the PZT as a rectangular wave. The full amplitude of the input voltage V_{in} is 150 V, and the input frequency f is 62 to 65 kHz, which corresponds to the natural frequency of the horn/PZT system. The oscillation of the PZT is amplified with an axi-symmetric step type horn. The total length of the horn is 36 mm, and the large and small end diameters are 30 mm and 15 mm. The amplification factor of the oscillation is proportional to the area ratio of the large and small ends of the horn, which is 4.0 in the present study. In order to increase the fuel flow rate, two narrow gutters are machined on the surface of the small end [6, 8].

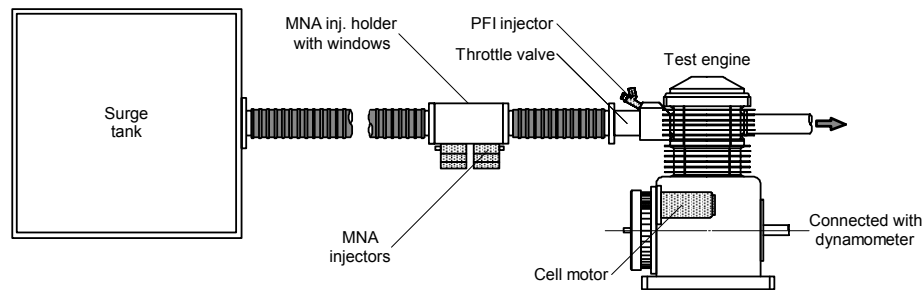
Figure 2 shows a schematic of the micro nozzle array. The micro nozzle array is set at the small end of the horn. The micro nozzle array is made of nickel film whose thickness is 30 μm , on which μm -order converging round nozzles are machined with the spacing of 70 μm . The nozzle exit diameter $d = 4$ and 6 μm , and the number of micro nozzles that attach the horn surface is 4.2×10^4 . Gasoline is periodically pushed out through the micro nozzles by the oscillation of the horn, and a fine uniform-diameter spray is formed.

Table 1 shows the test engine specifications. An air cooled, single cylinder, 4 stroke cycle gasoline engine is utilized. The stroke volume is 337 cm^3 , and the compression ratio is 8.0. Regular gasoline is used as the test fuel. The spark timing is controlled at arbitrary crank angles with an in-hose electronic circuit. The fuel injection start timing and duration are controlled automatically according to the air flow rate, the engine speed, and the target air fuel ratio (A/F) with an in-hose electronic control unit (ECU).

Figure 3 shows a schematic of the experimental setup for cold start experiments. Air is introduced into a surge tank through a round orifice, where a differential pressure gage is installed and the air flow rate is measured. The intake air is introduced to the test engine through a 1000 mm length flexible duct. MNA injectors are installed 400 mm upstream from the intake valve. In order to prevent the micro nozzle array from being broken due to the

Table 1. Test engine specifications.

Type	Air cooled, single cylinder, 4 stroke cycle, spark ignition
Stroke volume (Bore x stroke)	337 cm ³ (82 mm x 64 mm)
Compression ratio	8.0
Valve arrangement	Overhead valves (Intake: 1, Exhaust: 1)
Combustion chamber geometry	Wedge
Fuel injectors	MNA injectors or PFI injector
Fuel	Regular gasoline

**Figure 3.** Schematic of experimental setup for cold start experiment.

pressure pulsation, the MNA injectors are installed upstream of the throttle valve. The fuel is injected into the air flow in the perpendicular direction. In the MNA injector manifold, optical windows are installed in order to observe the spray formation. The PFI injector is installed 100 mm upstream from the intake valve. The PFI injector is installed between the throttle and intake valves. The fuel is injected so that the fuel spray impinges onto the intake valve. For both injectors, the fuel injection start timing is set at 10 deg ATDC in the expansion stroke, and the fuel injection duration is controlled automatically with the ECU.

Table 2 shows the procedure of the cold starting experiment. In order to ensure the reproducibility of the data, all the sequence, namely the cell motor start, the ECU start, the fuel injection start, and the fuel injection stop, are processed automatically using the ECU. After operation, the first ignition cycle is analyzed. The definition of the first ignition cycle is as the followings. The fuel injection starts at the 16th cycle of the procedure. Since the fuel injection start timing is set at 10 deg ATDC in the expansion stroke, the first injected fuel comes into the cylinder in the next cycle, namely the 17th cycle. If the ignition takes place at the 17th cycle, 'the first ignition cycle is defined to be 0th cycle from the fuel injection start'. For example, if the ignition takes place at the 19th cycle, the first ignition cycle becomes 2nd cycle. For MNA injectors, since the injectors are set at 400 mm upstream of the intake valve, a few more cycles are necessary until the injected fuel comes into the cylinder. For MNA injectors, the delay of the fuel arrival is taken into account when analyzing the first ignition cycle. Table 3 shows the experimental conditions. Cold start conditions of modern 4 stroke cycle gasoline engines are simulated as possible.

Results and Discussions

Figure 4 shows droplet size distributions. Figures 4 (a), (b), and (c) show the results for the PFI injector, MNA injector ($d = 6 \mu\text{m}$), and MNA injector ($d = 4 \mu\text{m}$), respectively. The vertical axis indicates the frequency, and the horizontal axis the droplet diameter. In these figures, the results at the spray axis ($z/D = 0.0$), and spray boundary ($z/D = 0.47$ to 0.5) are shown. In Figure 4 (a), for the PFI injector, it is observed that the peak diameter is around 15 to 20 μm , and most droplets are smaller than 50 μm . At the spray boundary ($z/D = 0.5$), large droplets whose diameter is 50 to 150 μm are seen. In Figure 4 (b), for MNA injector ($d = 6 \mu\text{m}$), the peak diameter is around 10 μm , and most droplets are smaller than 30 μm . At the spray axis, the secondary peak is observed around 25 μm , which can be attributed liquid film formation on the micro nozzle array surface [5-8]. In Figure 4 (c), for MNA injector ($d = 4 \mu\text{m}$), the peak diameter is around 8 to 10 μm , and most droplets are smaller than 20 μm . The droplet size distributions are similar at the spray axis ($z/D = 0.0$) and spray boundary ($z/D = 0.47$). The droplet size is uniform regardless of the measurement position [5-8].

Table 2. Procedure of cold starting experiment.

Cycle number	Events
Before operation	⇒ Data input to ECU. - Room temp., relative humidity, atm. press. are input. - Target air fuel ratio is input.
1	⇒ Cell motor starts.
↓	- Waiting for the engine speed to be constant.
11	⇒ ECU starts.
↓	- Surge tank press., engine speed, in cylinder press. are acquired.
↓	- No fuel injection signal is output.
16	⇒ Fuel injection starts.
↓	- Surge tank press., engine speed, in cylinder press. are acquired.
↓	- Fuel injection period is calculated, and fuel injection signal is output.
First ignition	⇒ Fuel injection stops. - When ignition is detected, fuel injection stops.
After operation	⇒ Data are stored in HDD. - From acquired data, first ignition cycle is analyzed.

Table 3. Experimental conditions.

Engine speed	350 rpm
Volumetric efficiency	$\eta_v = 0.60$
Spark timing	0 deg ATDC
Fuel injection start timing	10 deg ATDC in expansion stroke
Room temperature T_r	$T_r = 12 \pm 3 \text{ }^\circ\text{C}$
Engine head temperature T_h	$T_h = 18 \pm 3 \text{ }^\circ\text{C}$

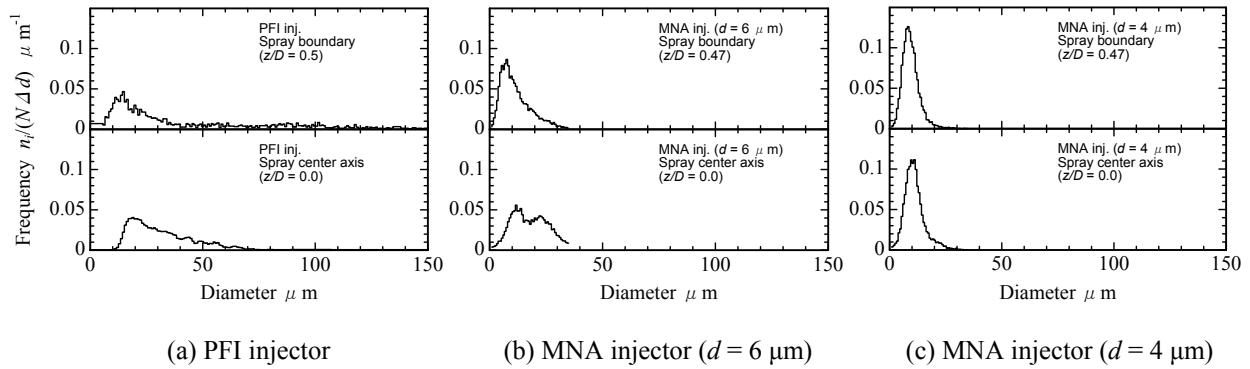
**Figure 4.** Droplet size distributions.

Figure 5 shows SMD distributions. The vertical axis indicates the SMD, and the horizontal axis the measurement position. Average SMDs are also indicated in the figure, which is estimated based on the local SMD and the local mass flux of the fuel. For the PFI injector, the local SMD is the smallest at the spray axis, and it increases at the spray boundary. The average SMD is 59 μm . For the MNA injector ($d = 6 \mu\text{m}$), the local SMD is slightly larger at the spray axis than that at the spray boundary. The average SMD is 23 μm . For the MNA injector ($d = 4 \mu\text{m}$), the local SMD is uniform regardless of the measurement position. The average SMD is 15 μm .

Figure 6 shows the relationship between the air fuel ratio A/F and the first ignition cycles from fuel injection start. Figures 6 (a), and (b) show the results for MNA injector ($d = 6 \mu\text{m}$), and MNA injector ($d = 4 \mu\text{m}$), respectively. The results for the PFI injector are also indicated in both figures for comparison. The vertical axis indicates the first ignition cycles, and the horizontal axis the air fuel ratio A/F . At each air fuel ratio, cold start experiments are carried out 18 times at maximum. If the first ignition cycle is no earlier than 25th cycle, the results are not indicated in these figures.

For the PFI injector, with the increase in the air fuel ratio A/F , the first ignition cycle becomes later and the scattering of the data becomes larger. Some portion of the injected fuel adheres to the intake port, intake valve, and in-cylinder walls as liquid films. Even at the stoichiometric condition, i.e. $A/F = 14.7$, the first ignition cycle is from 11th to 21st cycles. It is considered that the air fuel ratio of the gas phase is much leaner than that of global air fuel ratio.

In Figure 6 (a), results for the MNA injector ($d = 6 \mu\text{m}$) are indicated. Due to the limit of the fuel flow rate, experiments are carried out under conditions of $A/F < 4.9$. For the MNA injector ($d = 6 \mu\text{m}$), the first ignition cycle becomes later than that for the PFI injector, though the droplet diameter for the MNA injector ($d = 6 \mu\text{m}$) (average SMD = $23 \mu\text{m}$) is much smaller than that for the PFI injector (average SMD = $59 \mu\text{m}$). It is observed that, in the MNA injector manifold, injected spray impinges onto the inner wall due to the penetration and adheres as a liquid film.

In Figure 6 (b), results for the MNA injector ($d = 4 \mu\text{m}$) are indicated. Due to the limit of the fuel flow rate, experiments are carried out under conditions of $A/F < 9.8$. For the MNA injector ($d = 4 \mu\text{m}$), the first ignition cycle becomes earlier than that for the PFI injector. The droplet diameter for the MNA injector ($d = 4 \mu\text{m}$) (average SMD = $15 \mu\text{m}$) is much smaller than that for the PFI injector (average SMD = $59 \mu\text{m}$). It is observed that, in the MNA injector manifold, injected spray does not impinge onto the inner wall.

Figure 7 shows the relationship between the air fuel ratio A/F and the cumulative fuel amount $m_{f, \text{cumulative}}$. The definition of the cumulative fuel amount $m_{f, \text{cumulative}}$ is as the followings.

$$m_{f, \text{cumulative}} = \begin{cases} \sum_{i=0}^{n-1} m_{f,i} + m_{f,n} \frac{(A/F)_{\text{stoich}} - A/F}{(A/F)_{\text{stoich}}} \cdots A/F < 14.7 \\ \sum_{i=0}^{n-1} m_{f,i} \cdots A/F > 14.7 \end{cases} \quad (1)$$

where, $m_{f,i}$ is fuel injection mass at the i th cycle. The first term on the right hand side indicates the total amount of the injected fuel before the first ignition. The second term on the right hand side (only for $A/F < 14.7$) indicates the unburned fuel amount in the first ignition cycle. Note that for $A/F < 14.7$, not all the injected fuel is burned during the combustion process, and the cumulative fuel amount $m_{f, \text{cumulative}}$ cannot be zero even if the first ignition cycle is 0th cycle. Here, it is assumed that the combustion efficiency is 100 % (all the oxygen molecules in the cylinder are consumed) and that the air fuel ratio in the gas phase is also $A/F < 14.7$. Therefore, the cumulative fuel amount $m_{f, \text{cumulative}}$ underestimates the actual unburned fuel amount in the first ignition cycle.

In Figure 7, for the PFI injector, the cumulative fuel amount $m_{f, \text{cumulative}}$ takes the minimum value around $A/F = 7$ to 8. With the decrease in the air fuel ratio A/F , the first ignition cycle becomes earlier. However, the unburned fuel amount during the combustion process increases, and as a result, the cumulative fuel amount $m_{f, \text{cumulative}}$ increases. On the contrary, with the increase in the air fuel ratio A/F , the first ignition cycle becomes later. Therefore, the total amount of the injected fuel before the first ignition increases, and as a result, the cumulative fuel amount $m_{f, \text{cumulative}}$ increases. In the present study, the optimum air fuel ratio A/F at cold starting is around 7 to 8, and the minimum value of the cumulative fuel amount $m_{f, \text{cumulative}}$ is 115 mg.

In Figure 7, for the MNA injector ($d = 6 \mu\text{m}$), the cumulative fuel amount $m_{f, \text{cumulative}}$ is larger than that for the PFI injector, which can be attributed to that the first ignition cycle is later. The droplet diameter for the MNA injector ($d = 6 \mu\text{m}$) (average SMD = $23 \mu\text{m}$) is much smaller than that for the PFI injector (average SMD = $59 \mu\text{m}$).

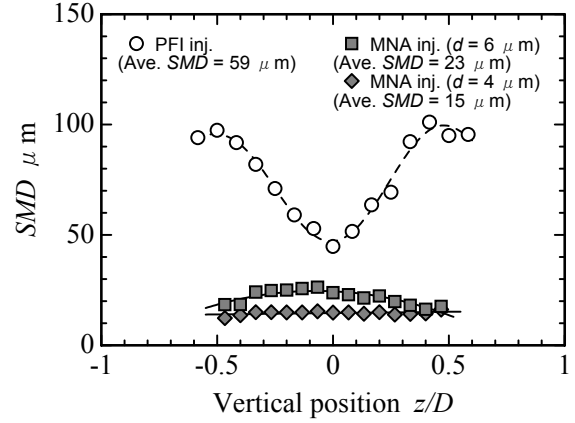


Figure 5. SMD distributions.

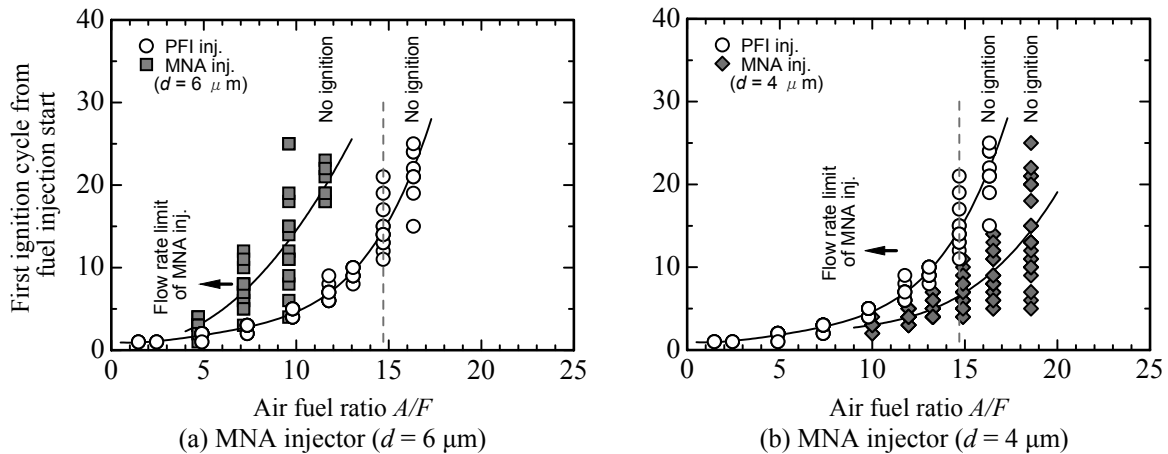


Figure 6. Relationship between air fuel ratio and first ignition cycles from fuel injection start.

However, due to the wall wetting in the injector manifold, the effect of the atomization improvement is killed. On the contrary, for the MNA injector ($d = 4 \mu m$), the cumulative fuel amount $m_{f, cumulative}$ is smaller than that for the PFI injector, which can be attributed to that the first ignition cycle is earlier. The droplet diameter for the MNA injector ($d = 4 \mu m$) (average SMD = $15 \mu m$) is much smaller than that for the PFI injector (average SMD = $59 \mu m$). Using such a fine spray, it could be possible to reduce the cumulative fuel amount $m_{f, cumulative}$. The minimum value of the cumulative fuel amount $m_{f, cumulative}$ is 84 mg, which is 30 % smaller than that for the PFI injector. It is shown that, by use of the MNA injector, UHC emissions at cold starting of a 4 stroke cycle gasoline engine can be reduced.

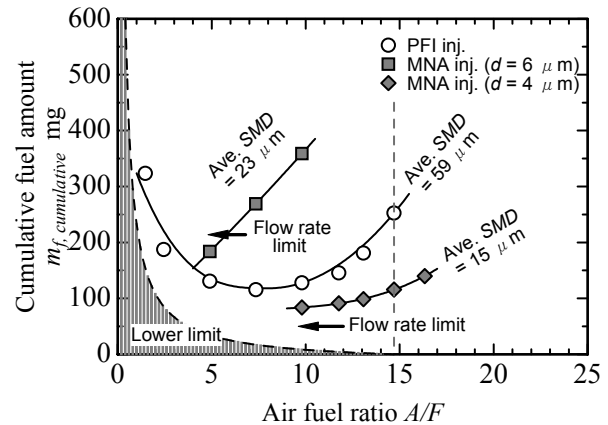


Figure 7. Relationship between air fuel ratio and cumulative fuel amount.

Acknowledgements

The present study is carried out as a cooperative research between Toyota Motor Corporation and Gunma University. The authors thank Seichin KINUTA of Optics Precision Co., Ltd., Hongyu YANG, Satoshi HARA and Hisao NAKAMURA of Gunma University for their help in experimentation.

References

1. Takahashi, Y. et al., *Proc. FISITA2006*, Paper No. F2006P106, 2006.
2. Cheng, W. K. et al., *SAE Paper 932708*, 1993.
3. Witze, P. O. and Green R. M., *Proc. 8th Int. Symp. Applications of Laser Techniques to Fluid Mechanics*, 1996, pp.13-3-1 – 13-3-8.
4. Witze, P. O. and Green R. M., *SAE Paper 970866*, 1997.
5. Araki, M. et al., *Trans. the Japan Society of Mechanical Engineers (Series B)*, Vol.73, No.726, 2007, pp.622-630.
6. Araki, M. et al., *Trans. the Japan Society of Mechanical Engineers (Series B)*, Vol.74, No.737, 2008, pp.228-236.
7. Araki, M. et al., *Proc. the 10th Int. Conf. Liquid Atomization and Spray Systems (ICLASS 2006) (CD-Rom)*, 2006.
8. Araki, M. et al., *SAE Paper 2007-32-0050*, 2007.
9. Iki, N. et al., *Proc. the 13th Symposium (ILASS-Japan) on Atomization*, 2004, pp.201-204.
10. Shimakawa, S., *Ultrasonic Engineering*, 1975, Kogyo Chosakai Publishing, pp.118-122.
11. Matsuo, T. et al., *Journal of Society of Automotive Engineers of Japan*, Vol.59, No.2, 2005, pp.39-43.